THE SEMIANNUAL REPORT OF THE MSU GROUP

(Jan.-Jun. 1998)

Contributors: V.B.Braginsky (P.I.), I.A.Bilenko, M.L.Gorodetsky,
F.Ya.Khalili, V.P.Mitrofanov, K.V.Tokmakov, S.P.Vyatchanin,
Collaboration with the theoretical group of prof. K.S.Thorne

I. SUMMARY

A. Excess noise in steel suspension wires for the laser gravitational wave detector (I.Bilenko, A.Ageev)

The progress on the mechanical excess noise research is reportred. The improved technique of wire oscillation measurement has been applied to the extended investigation of steel test mass suspension for the GW detector.

The sensitivity of measurements has been improved up to 10 times and reached the value of displacement resolution

$$\Delta x_{min} \simeq 2 \times 10^{-11} cm/\sqrt{Hz}$$

We were working with the wires of 80 and 90 μm in diameter provided by the LIGO team. About 100 hours of noise intensity records have been made which allow us to make some conclusions about the properties of the material. The dependence of the excess noise intensity in fundamental violin mode of the steel wires on the stress value is obtained. The excess noise becomes significant when the stress is approximately 70% of breaking tension or higher. The intensity and magnitude of spontaneous amplitude variations for all tested samples was substantially smaller than that earlier obtained in tungsten wires. In contrast with the experiments with tungsten we observed no large bursts as compared with the average thermal amplitude motion amplitude. The variations of the amplitude during the time intervals of $0.2s$ (short as compared with the ringdown time of the wire) overcome rms value

up to times per hour (which is not related to pure Brownian motion with the probability $P \geq 0.997$).

Our explanation is the more homogeneous inner structure of steel in comparison with tungsten. Hence, the application of amorphous material seems highly advantegeous. The design of the expewrimental system for noise measurement on fused silica suspension is in progress now.

It was confirmed that the statistic of the noise varies significantly from sample to sample, which is the result of nonuniform distribution of noise sources along the wire rolls.

The excess noise observed on the steel wires could be neglected on the inithial LIGO stage if the coinsidence observations on two or more interferometers will be realised. However, it could case a serious problem for the advanced LIGO project.

The detailed description of the experimental installation and the full set of the experimental results see in the Appendix A.

B. The method of reduction of the suspention thermal noise (S.P.Vyatchanin in collaboration with Yu.Levin from K.Thorne's group)

The suspension noise in interferometric gravitational wave detectors is caused by losses at the top and the bottom attachments of each suspension fiber. We use the Fluctuation-Dissipation theorem to argue that by careful positioning of the laser beam spot on the mirror face it is possible to reduce the contribution of the bottom attachment point to the suspension noise by several orders of magnitude. For example, for the initial and enhanced LIGO design parameters (i.e. mirror masses and sizes, and suspension fibers' lengths and diameters) we predict a reduction of ~ 100 in the "bottom" spectral density throughout the band $35 - 100$Hz of serious thermal noise.

We then propose a readout scheme which suppresses the suspension noise contribution of the top attachment point. The idea is to monitor an averaged horizontal displacement of the fiber of length l; this allows one to record the contribution of the top attachment

point to the suspension noise, and later subtract it from the interferometer readout. This method will allow a suppression factor in spectral density of 0.92 $(l/d^2)\ \sqrt{Mg/\pi E}$, where d is the fiber's diameter, E is it's Young modulus and M is the mass of the mirror. For the test mass parameters of the initial and enhanced LIGO designs this reduction factor is $132 \times (l/30\text{cm})(0.6\text{mm}/d)^2$.

We offer what we think might become a practical implementation of such a readout scheme. We propose to position a thin optical waveguide close to a fused silica fiber used as the suspension fiber. The waveguide itself is at the surface of a solid fused silica slab which is attached rigidly to the last mass of the seismic isolation stack. The thermal motion of the suspension fiber is recorded through the phaseshift of an optical wave passed through the waveguide. A laser power of 1mW should be sufficient to achieve the desired sensitivity.

This work was done in collaboration between MSU group and Caltech Theoretical astrophysics group.

C. The improvement of the Q factors of the suspensions' modes (V. Mitrofanov K. Tokmakov, N.Styazhkina)

Valery Mitrofanov and Kirill Tokmakov have finished the implementation of new systems for exciting and monitoring pendulum oscillation of the test mass in new vacuum chamber aimed to reach Q for the suspensions' pendulum and violin modes greater than 3×10^8. Optical sensor based on transformation of the oscillation amplitude into the time interval is used to monitor the change of amplitude in order to measure Q factors. Before testing of new suspensions they have investigated the effect of fused silica vapor sedimentation on surface of the fibers in the process of fabrication. Using these studies they suggested to change the technique of welding of fused silica fibers to the special pins on the test mass and the top plate of the support structure. These changes in the technique permit to reduce vapor sedimentation. They concern a choice of temperature at which welding is performed, a choice of the size of the pin and thick part of the fused silica fiber to be welded, as well as

setting of screen on the fiber when it is welded. The fabrication of new test mass suspensions for their testing is in progress.

V. Mitrofanov and post graduate student Natasha Styazhkina continued the study of electric field damping in the test mass oscillations. The reductions of the electric field losses is important for the development of the electric actuators. They have found that the electric losses depend significantly on the thermal treatment of the conductive surfaces on the test mass and the electrode to which electric field is applied.

D. Quantum limits and symphotonic states in gravitational wave antennae on free masses (M.Gorodetsky, F.Khalili)

The new article is under preparation for publication. Here we present the main obtained results.

Quantum mechanics sets strict frames on the sensitivity and the required circulating energy in traditional gravitational wave antennas on free masses. The possible way out is to use intracavity QND measurements. In this paper we analyzed a new QND observable and corresponding symphotonic quantum states, possessing a number of features which make them promising for experiments where registration of small variations of phase are required:

1) Unlike other known QND observables, this one is a joined integral of motion for two quantum oscillators with equal frequencies.

2) Crossquadrature observable has high sensitivity to phase difference of the oscillators. Phase difference of the order of $1/N$ (theoretical limit for phase measurements) may be detected, where N - is number of quanta in the system.

3) To measure this new observable well known methods of QND measurement of electromagnetic energy may be used.

We considered practical optical scheme in which the new observable may be used for the detection of gravitational waves.

As estimates show in combination with advanced coordinate meters this scheme provides

the sensitivity of the same order as in planned antennas at signficantly lower energies.

Summing up the results of this article and the previous ones (see annual reports 1997 and 1996) we may conclude that intracavity measurements with automatically organizing nonclassical optical quantum states allow in principle to lower levels of required power and in several cases to achieve sensitivity better than the SQL.

It is also appropriate to note here that the schemes we analyzed do not cover all possible geometries of intracavity measurements. Better realizations with higher response are probably possible.

APPENDIX A: EXCESS NOISE IN STEEL SUSPENSION WIRES FOR THE LASER GRAVITATIONAL WAVE DETECTOR (A.YU.AGEEV, I.A.BILENKO, V.B.BRAGINSKY)

The progress on the mechanical excess noise research is reported. The improved technique of wire oscillation measurement has been applied on the investigation of a test mass suspension for the GW detector. The dependence of excess noise intensity in fundamental violin mode of the steel wires on the stress value is obtained.

1. Introduction

The goals of LIGO project are to reach the sensitivity which will be sufficient to detect and to record in details the bursts of gravitational radiation produced by astrophysical catastrophes far away from our galaxy [1,2]. At the first stage the gravitational antennas has to reach the resolution in the units of the perturbation of metric at the level $h \simeq 10^{-21}$. In the following stages the sensitivity has to be higher. The mechanical noise which will influence the movement of the antenna test masses and thus will limit the sensitivity are of fundamental importance in this project. Usually to describe the mechanical noise of the mirrors the classical model of the Brownian motion is used [3,4]. In this model the statistic of random mechanical pulses which act on the mirrors and thus may mimic the gravitational

wave bursts is in essence the Gaussian one. It means that with the rise of a certain threshold the event rate of the pulses falls exponentially. On the other hand it is reasonable to expect the existence of nonbrownian noise (excess noise) produced by the redistribution of defects in the stressed suspension of test masses. In our previous paper [5] we reported the observation of the excess noise in tungsten wires. In these experiments we observed two types of excess noise: spontaneous rise of the intensity of the noise during certain finite time intervals and random jumps of amplitude. The event rate of the jumps correlated with the value of applied mechanical stress. The relatively high level of observed excess noise may be explained by strong inhomogenity of wires tungsten. In this paper we present our resent results of the observation of the excess noise in the steel wires with much smaller size of crystallines. This material was provided us by the LIGO team. The identical wires will be used for mirror suspension in the first srage of LIGO project.

2. Experimental setup

The laser interferometric device prepared formerly for the excess noise measurement has been used. An essential improvement of the experimental installation and the method of measurement have been made in comparison with the first one in which the tunsten wires have been examined. The amplitude of Brownian oscillation on the fundamental violin mode of a string is:

$$\bar{A} = \sqrt{\frac{2kT}{m^*\omega^2}} \qquad \text{(A1)}$$

Here ω is violin mode frequency, k is Boltzman constant, T is temperature and m^* is effective mass of the string. For the steel wires $l = 15\ cm$ long and 80 μm in diameter under the stress about 50% of breaking tension the value $\omega \simeq 2\pi \times 1.5\ kHz$ and the value of $\bar{A} \simeq 2 \times 10^{-10}\ cm$. This value is approximately 3 times smaller than in the previous experiments with the 80 μm diameter tungsten wires.

We had managed to increase the sensitivity of the measurements up to 10 times and reached the value of displacement resolution

$$\Delta x_{min} \simeq 2 \times 10^{-11}\ cm/\sqrt{Hz} \qquad \text{(A2)}$$

The key feature of the new installation is the possibility of parallel observations on the two different samples placed in the ends of two arms of the interferometer (see *Figure* 1). It allows one to vetoe any external disturbances which may appear due to residual seismic and laser power fluctuations using an anticorrelation method. In additional, the enhanced feedback stabilization scheme have kept the perfect tuning of the interferometer during up to $10 - 14$ hours, which allows to make a long time records. A new calibration method has been used. We used the $He - Ne$ laser wavelength as a reference. The beam splitter was attached to PZT drive, which could be driven by the AC source on the frequency close to the fundamental mode frequencies of the tested wires. When the amplitude of the beam splitter oscillation reaches the quarter wave value, the output signal on this frequency becomes specifically distorted. Reducing the AC value till the response of the system becomes equal to the signals corresponded to the wires oscillations one can determine these amplitudes with sufficient accuracy. At the same time the linearity of the system is tested. In the process of measurements the PZT drive was used by feedback stabilization scheme for the compensation of slow drift in the interferometer.

In this report the results obtained on the steel samples 15 cm length 80 μm in diameter under the stresses from 50% to 95% from the breaking tension value are presented. All the samples had been polished and cleaned before measurement. The breaking tension value has been determined in the set of the preliminary tests as the ratio of the critical load value to the cross-section area of the samples. Critical load produces the break of the samples during 1-3 seconds.

Each sample was clamped on the frame of experimental device once for all measurements. However, it was possible to change its stress from one measurement to another. The minimum interval between the measurements was $3 - 4$ *hours* because this process requires the vacuum chamber to be open. In contrast with the previous experiments with tungsten only the top end of the sample was fixed. The bottom end was attached to the lead load.

To prevent the horizontal movement of the load it was fixed by the thin cantilever made of bronze. The bending rigidity of the cantilever was small in comparison with the longitudinal rigidity of the sample. As a result, the sample was subjected to the constant stress on the same way as the suspension wires of the antenna mirrors.

The signal on the detector output contains the spectral components corresponding to the oscillations of two different samples. A separation of the components was possible due to the difference of its frequencies. It was based on the real time fast Fourier transform. The results of each experiment were the records of the amplitude and frequency for the two samples. Each value was a result of averaging over 0.2 sec ($180 - 400$ periods of oscillation for the frequencies $0.9 - 2.3$ kHz, typical for the stress values mentioned above). Hence, the effective bandwidth defined by 1024 points FFT was 0.5 Hz. The signal-to-noise ratio in this bandwidth was $5 - 12$, which allows to observe the random changes of the amplitude during the time interval shorter than the relaxation time τ^* of the samples oscillations (typically $5 - 12$ sec).

3. Experimental results

The analysis of the results consisted of two different approaches. First one was based on the amplitude averaging over the time interval $t = 3 \times \tau^*$. The obtained values A_t can be regarded as independent realizations of a stochastic process. The variation of these values is denoted σ_{At}. These amplitudes have been compared with $\bar{A}$ in order to select statistically significant deviations. The χ^2 criterion has been used. We observe relatively short $(1 - 3\tau^*)$ rising of the amplitude up to the $3 - 4$ σ_{At} level happens up to 20 times per 10 hours of observation, that in some cases was a statistically significant exceedence of the Brownian motion amplitude. It is important, that the measured mean amplitude over long time interval was always equal to the estimated value for the Brownian motion with the accuracy better than 15%. We have no reasonable explanation for this rising of the amplitude yet. Note, that the absence of any correlation between such events in the pairs of

samples may be regarded as the evidence of inner nature of such a behaviour of the samples.

The second approach treated the variations of the oscillation amplitude during the time shorter than the relaxation time. The ems value of the variations is:

$$\Delta A_{ems} \simeq \sqrt{\frac{2kT}{m^*\omega^2}}\sqrt{\frac{2t}{3\tau^*}} \tag{A3}$$

, where k is the Boltzman constant, T is the temperature m^* is the effective mass. If the violin mode ringing time $\tau^* = 10\ sec$, averaging time $t = 0.2\ sec$, $\Delta A_{ems} \simeq 0.12\bar{A}$. The variations of amplitude are independent realizations of a stochastic process. The distribution of these values for the pure Brownian motion has to be close to Gaussian. The distributions obtained in experiments show the excess quantity of the high variation of amplitude (see $table1$). The samples 1-5 were 80 μm in diameter, samples 6 and 7 were 90 μm. The number of such events varies from a few units to a few tens per 10 hours for the different samples. In many cases the number of the excessive events was statistically significant. The dependence of the excess event rate for 3 selected samples presented on the $figure2$. We choose a 3σ level as a threshold for this plot. The dependencies of the event rate on the threshold level for one sample under four different stresses are on the histograms (see $figure3$).

In additional the spectrum analysis of the amplitude records and crosscorrelation analysis of the records pairs have been done. No periodic excitations of the sample oscillation as well as pair correlation have been found. When the stress value was above $\simeq 90\%$ of breaking tension the slow decrease of the fundamental mode frequency during the experiment was observed. It corresponds to the viscous flow of the steel. For example, for the sample 5 under the maximum stress the speed of flow was:

$$\frac{1}{L}\frac{\partial L}{\partial t} \simeq 6 \times 10^{-5}\ 1/hours \tag{A4}$$

For the smaller stress value the speed of flow was less then the resolution limit of the method of measurement:

$$\frac{1}{L}\frac{\partial L}{\partial t} < 3 \times 10^{-6}\ 1/hours \tag{A5}$$

4. Discussion

The main conclusion from the results reported above is the existence of an excess noise in the fundamental violin mode oscillation of the well stressed steel wires. The intensity and magnitude of the spontaneous amplitude variations is substantially smaller than it was obtained earlier on the tungsten wires [5] . Possible explanation is the more homogeneous inner grain-like structure of the steel in comparison with the bamboo-like structure of the tungsten. The statistic of the noise varies significantly from sample to sample, which is an evidence of the nonuniform distribution of the noise sources within the samples. This variation was proved to be large enough to hide any details of the dependence of the excess noise on the stress value and other factors. The presence of the excessive peaks even in the samples which did not evince viscous flow means that its origin can not be explained by the model of mechanical shot noise [6] . The fast variation of the oscillation amplitude could be a result of avalanche-like process within the small part of the sample, which originally contains some type of inhonogenety. As far as our method of research does not provide information about fine time and space structure of the noise, it is difficult to develop any detailed model.

Let us evaluate the magnitude of the possible rapid (during the time about 1 ms) test mass displacement induced by the excessive variations of the Brownian oscillation amplitude of the suspension wire observed in the experiments. If this variation happens during the time smaller as compared to the oscillation period, the magnitude of test mass displacement should be maximal:

$$\Delta X \simeq \frac{2g}{l\omega^2}\Delta x = 1 \times 10^{-15}\ cm \qquad \text{(A6)}$$

here $\Delta x = 4 \times 10^{-10}\ cm$ is an instant variation of the oscillations amplitude, $l = 20\ cm$ - suspension length, $\omega = 2\pi \times 2 \times 10^3\ Hz$ - fundamental mode frequency. It means that under certain conditions the excess noise in suspension wires could generate the kicks acted on the test masses and simulated the signal bursts $h = \frac{\Delta X}{2L} \simeq 5 \times 10^{-21}$.

REFERENCES

[1] A.A. Abramovici et.al. Science **256** , 325 (1992)

[2] A.A. Abramovici et.al. Phys. letters A, **218** , 157 (1996)

[3] A.Gillespie, F.Raab Phys. letters A, **178** , 357 (1993)

[4] G.I.Gonzalez, P.R.Saulson Phys. letters A, **201** , 12 (1995)

[5] A.Yu.Ageev, I.A.Bilenko, V.B.Braginsky, S.P.Vyatchanin Phys. letters A, **227** , 159 (1997)

[6] G.Cagnoli, L.Gammaitoni, J.Kovalik, F.Marchesoni, M.Punturo Phys. letters A, **237** , 21 (1997)

FIGURES

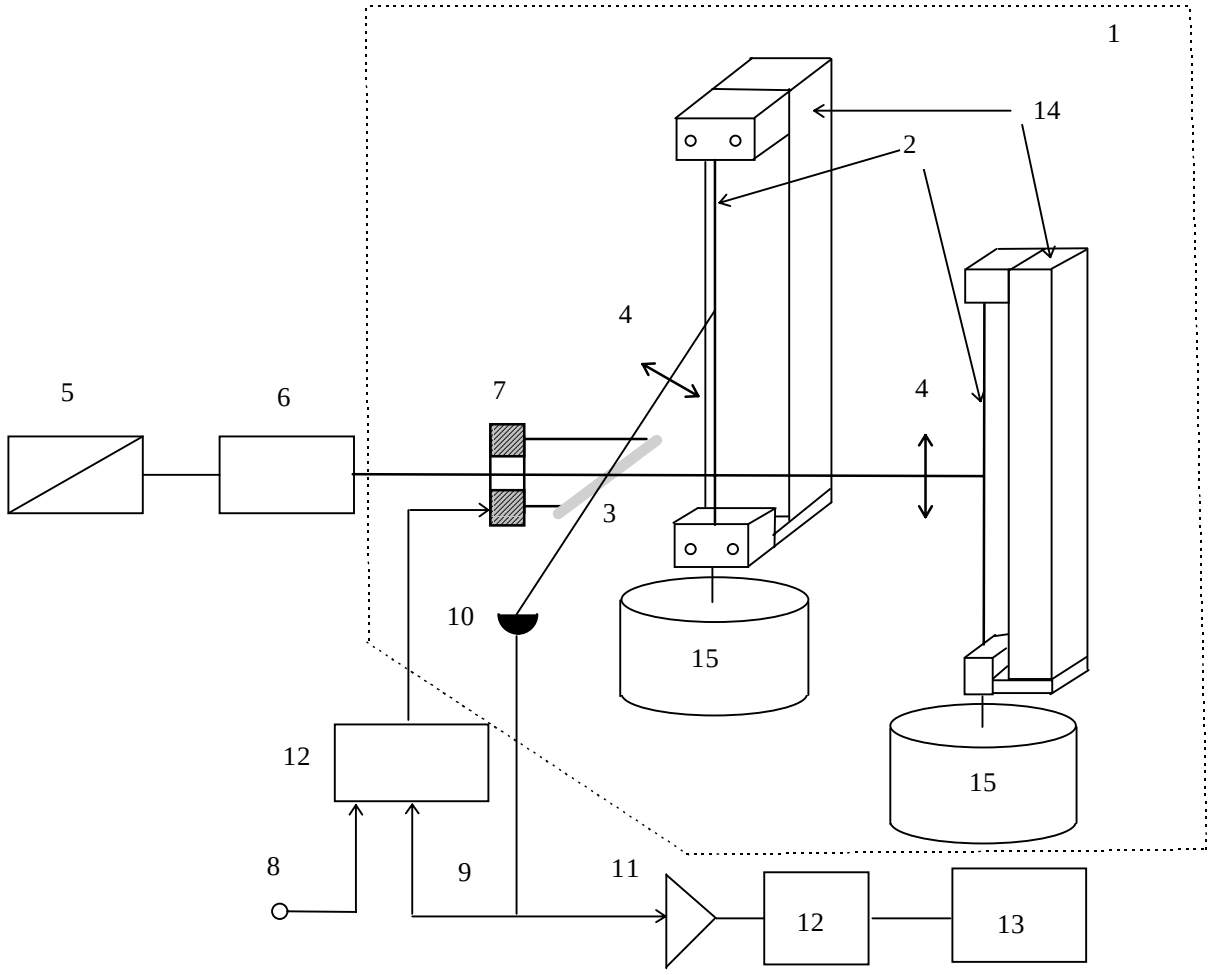

1. Vacuum chamber which contains fiber samples and readout interferometer.
2. Fiber sample.
3. PZT driven beam splitter.
4. Aspherical lens with a focal spot of 5 μm in diameter on fiber surface.
5. Helium-neon frequency-stabilised laser.
6. Optical insulator.
7. PZT drive.
8. Calibrating signal input.
9. Slow drift compensation loop.
10. Detector.
11. Low noise amplifier.
12. Band pass filter.
13. ADC.
14. Rigid frame for the fiber fixation.
15. Lead load.

Figure 1. Schematic diagram of the interferometric readout for the excess noise measurement.

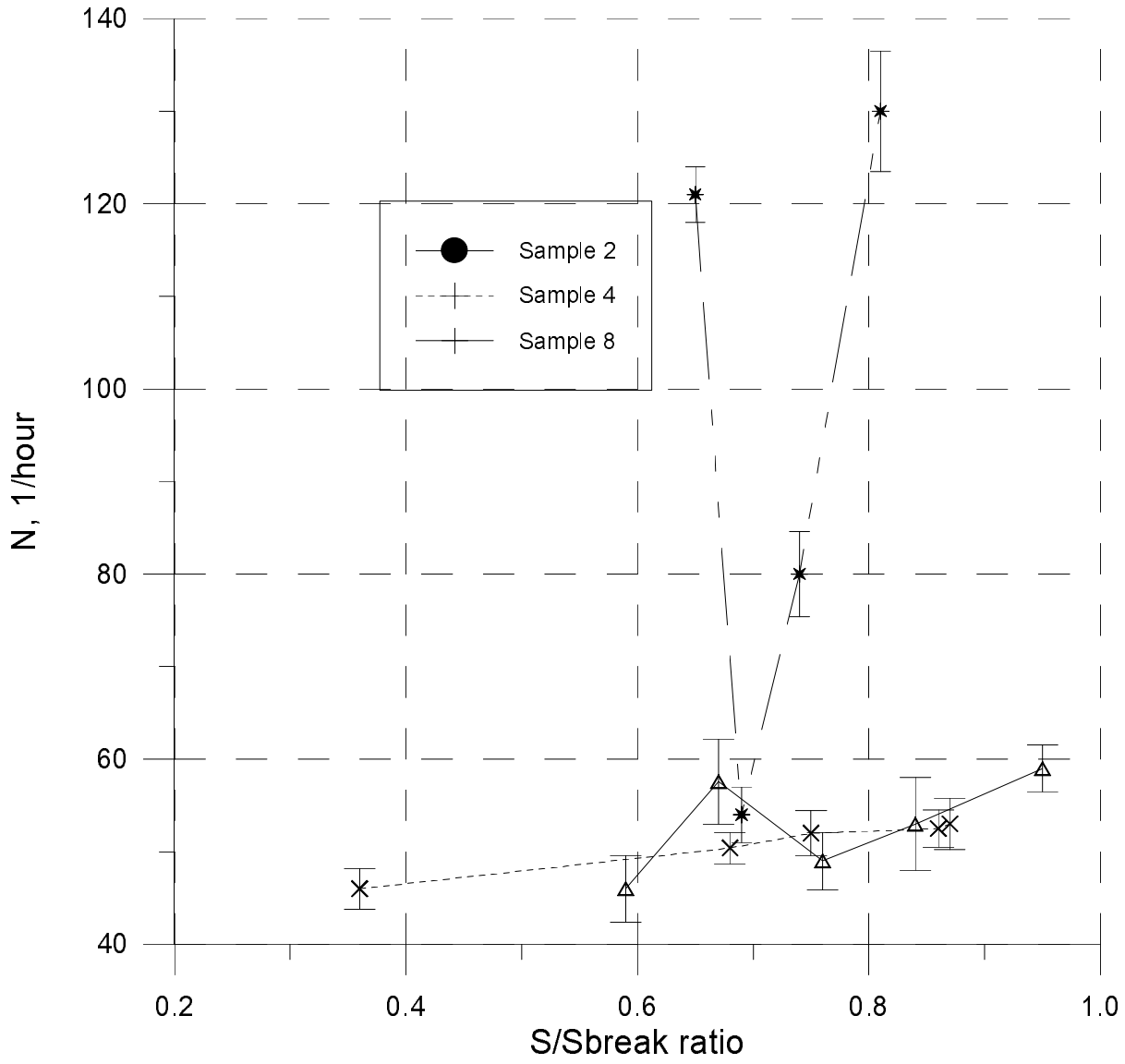

Figure 2
The dependence of the amplitude bursts
$\Delta A > 3\ \Delta A_{ems}$ intensity on the stress value

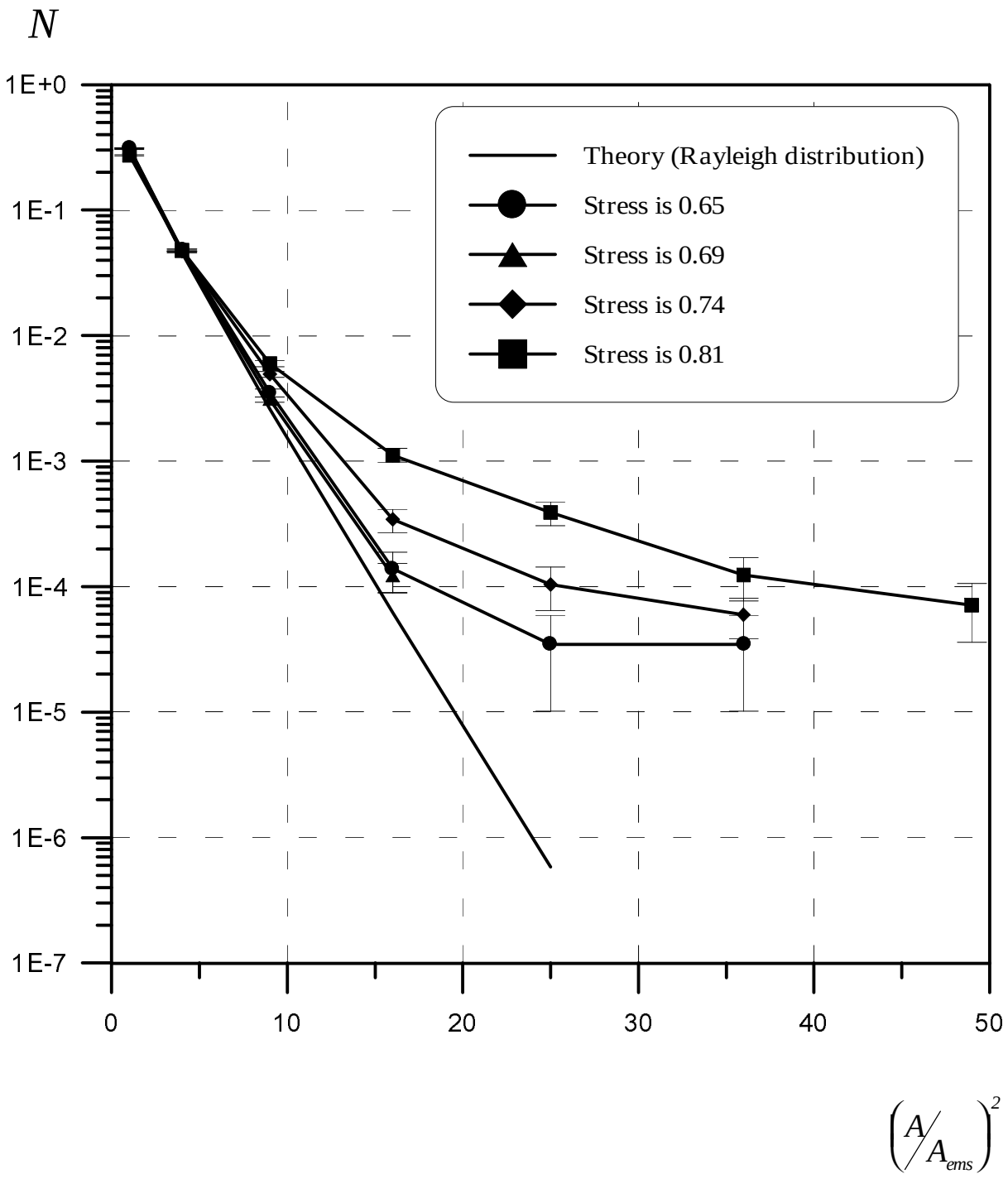

Figure 3. Peak intensity histogram.
N is the number of peaks per hour with amplitude exceeding A_{ems}.

6	5	1	4	4	4	4	2	7	8	8	8
1423	1428 (0.50)	1441 (0.51)	1653 (0.68)	1726 (0.74)	1856 (0.86)	1875 (0.87)	1955 (0.95)	2013 (0.65)	2078 (0.69)	2152 (0.74)	2256 (0.81)
12.3	16.24	9.25	16.3	8.89	12.9	6.7	9.25	12.9	6.4	3.7	3.1
54.1 (666) [576]	74 (1208) [760]	93.5 (865) [433]	50.4 (821) [763]	52 (463) [416]	52.5 (677) [603]	53 (355) [314]	59 (546) [433]	121 (1565) [603]	54 (345) [299]	80 (298) [175]	130 (403) [146]
1.6 (20) [14]	5.29 (86) [18]	12.4 (115) [10]	1.8 (29) [18]	1.8 (16) [10]	1.8 (23) [14]	2.1 (14) [7]	4.3 (40) [10]	17.4 (225) [14]	2.2 (14) [7]	6.5 (24) [4]	28 (87) [3]
0 (0) [0]	0.24 (4) [0]	0.76 (7) [0]	0.18 (3) [0]	0.1 (1) [0]	0.23 (3) [0]	0.75 (5) [0]	0.43 (4) [0]	2.6 (33) [0]	0.16 (1) [0]	2.4 (8) [0]	9 (28) [0]

Table 1
The exsess noise peaks event rate
observed on different steel samples

APPENDIX B: HOW TO REDUCE THE SUSPENSION THERMAL NOISE IN LIGO WITHOUT IMPROVING THE Q'S OF THE PENDULUM AND VIOLIN MODES. (V. B. BRAGINSKY, YU. LEVIN AND S. P. VYATCHANIN)

The suspension noise in interferometric gravitational wave detectors is caused by losses at the top and the bottom attachments of each suspension fiber. We use the Fluctuation-Dissipation theorem to argue that by careful positioning of the laser beam spot on the mirror face it is possible to reduce the contribution of the bottom attachment point to the suspension noise by several orders of magnitude. For example, for the initial and enhanced LIGO design parameters (i.e. mirror masses and sizes, and suspension fibers' lengths and diameters) we predict a reduction of ~ 100 in the "bottom" spectral density throughout the band $35 - 100$Hz of serious thermal noise.

We then propose a readout scheme which suppresses the suspension noise contribution of the top attachment point. The idea is to monitor an averaged horizontal displacement of the fiber of length l; this allows one to record the contribution of the top attachment point to the suspension noise, and later subtract it from the interferometer readout. This method will allow a suppression factor in spectral density of $(l/d^2)\sqrt{Mg/\pi E}$, where d is the fiber's diameter, E is it's Young modulus and M is the mass of the mirror. For the test mass parameters of the initial and enhanced LIGO designs this reduction factor is $132 \times (l/30\text{cm})(0.6\text{mm}/d)^2$.

We offer what we think might become a practical implementation of such a readout scheme. We propose to position a thin optical waveguide close to a fused silica fiber used as the suspension fiber. The waveguide itself is at the surface of a solid fused silica slab which is attached rigidly to the last mass of the seismic isolation stack (see Fig. 5). The thermal motion of the suspension fiber is recorded through the phaseshift of an optical wave passed through the waveguide. A laser power of 1mW should be sufficient to achieve the desired sensitivity.

1. Introduction

Random thermal motion will be the dominant noise source in the frequency band of $35 - 100$ Hz for the first interferometers [1] and in the frequency band of $25 - 126$ Hz for the enhanced interferometers [1] in the Laser Interferometer Gravitational Wave Observatory (LIGO) [2].

The thermal noise in this frequency band is caused by the losses in the suspension fibers, in particular at the top and the bottom of each fiber's attachment point. So far the only known way to reduce the thermal noise has been to improve the quality of the suspension fibers and their attachments. Here we suggest a different approach:

In Section II we will present a general analysis of the suspension noise based on a direct application of the Fluctuation-Dissipation theorem. We will explicitly separate the contributions to the thermal noise of the top and the bottom attachment points of the suspension fibers. It has been a common opinion that the top and bottom attachments contribute equally to the thermal noise. We shall challenge this point of view. In fact, we will show that if one shifts the laser beam spot down from the center of the mirror by an appropriately chosen distance h, the contribution of the bottom attachment point to the thermal noise can be reduced by several orders of magnitude. Fig. 3 presents plots of this reduction factor in the frequency band 35–100Hz for three different choices of h. What is plotted here is the ratio $S_{\rm bottom}(f)/S_{\rm top}(f)$, where $S_{\rm bottom}(f)$ and $S_{\rm top}(f)$ are the spectral densities of thermal

---

[1] To be specific, we refer to the step 4 of LIGO enhancement — see [2]. In these the suspension thermal noise was calculated assuming the structural damping mechanism. However, the nature of dissipation in fused silica (e.g. viscous vs structural) is not yet fully established for the above frequency bands.

[2] The analysis of this paper is fully applicable to all other Interferometric Gravitational Wave detectors (e.g. VIRGO, GEO-600, TAMA etc.). For the sake of brevity in this paper we will refer only to LIGO.

noise contributed by the bottom and the top attachment points respectively. All three values of h are close to

$$h = \frac{I}{M(R+l)} \tag{B1}$$

[cf. Eq(B14)], where l is the length of the suspension fiber, I is the test-mass moment of inertia for rotation about the center of mass in the plane of Fig. 1 (see later), R is the radius of the mirror face and M is the mass of the test mass. The numerical values of these parameters for the initial and enhanced LIGO interferometers are

$$M = 10\text{kg}, \quad l = 30\text{cm}, \quad R = 12.5\text{cm}, \tag{B2}$$

$$I = 4.73 \times 10^5 \text{g cm}^2, \quad h = 1.11\text{cm}.$$

Out of the three graphs presented in Fig. 3 the one with $h = 1.0$cm seems to be the optimal one. From the graphs we see that reduction factors of $\simeq 10^{-2}$ in the "bottom" component of the thermal noise is possible over the entire band of serious thermal noise: 35 to 100 Hz.

In Sec. IIIA we concentrate on the top attachment point. Lossy defects at the top create noise not only in the test mass motion, but also noise in the motion of the fiber. The latter is significantly larger than the former — by a factor of order $f^2/f^2_{\text{pendulum}}$ at frequencies above the pendulum frequency and below the violin resonances (which are the frequencies of interest for LIGO thermal noise). We show that if one monitors the average horizontal displacement of the suspension fiber of length l, one can essentially record the fluctuating "driving force" originating at the suspension top, and then subtract it from the interferometer's readout, thereby reducing thermal noise originating at the suspension top. The reduction factor in the spectral density of thermal noise is given by $P = 0.93 \cdot l/\lambda$ [cf. Eq(B26)]. Here

$$\lambda = (d^2/8)\sqrt{\pi E/Mg} \tag{B3}$$

is the length of the segment of fiber near it's top where the bending is greatest, d is the fiber's diameter, E is the fiber's Young modulus and g is the acceleration of gravity. For a fused silica fiber of diameter $d = 0.6$mm one gets a thermal noise reduction factor of $P \simeq 132$.

In Sec. IIIB we offer a particular way of implementing such a procedure. The basic idea is shown in Fig. 5. A fused silica slab is rigidly attached to the "ceiling" (i.e. to the last mass of the seismic isolation stack), and a waveguide ab is carved into the slab's surface. A monochromatic optical wave is set up in the waveguide, and a fused silica fiber used as the suspension fiber is positioned close to the waveguide, within the optical wave's evanescent field. When the fiber is displaced relative to the waveguide, it will change the optical wave's propagation speed, thus inducing an overall phaseshift of the wave. The detailed calculations in Sec. IIIB show that $\sim$ 1mW of optical power in the wave is sufficient to reach the required sensitivity.

2. How to reduce thermal noise originating at the bottom attachment point

a. The model and formalism

The particular suspension that we consider is sketched in Fig. 1. We consider a compact rigid test mass of mass M suspended by a single fiber of length l and mass m; the fiber's bottom end is attached, for concreteness, to the top of the test mass (the main conclusions of this paper are also valid when the test mass is suspended by a fiber loop, as is planned for LIGO).

References [3], [4], [5], [7] give detailed explanations of how to use the Fluctuation-Dissipation theorem directly (without normal-mode decomposition) to calculate the spectral density of thermal noise [3]. In what follows we use the approach elaborated in [7].

To calculate the spectral density $S_{\rm x}(f)$ of suspension's thermal noise at frequency f we imagine applying an oscillating force F perpendicular to the test mass's mirror surface at the center of the readout laser beam spot [4]:

---

[3]The original formulation of the Fluctuation-Dissipation theorem is given in [6]

[4]This prescription is only valid when the test masses are perfectly rigid, which is a good approxi-

$$F(t) = F_0 \cos(2\pi f t). \tag{B4}$$

Then S_x is given by [cf. Eq (3) of [7]]

$$S_x(f) = \frac{2k_B T}{\pi^2 f^2} \frac{W_{diss}}{F_0^2}, \tag{B5}$$

where W_{diss} is the average power dissipated in the system (suspension, in our case) when the force $F(t)$ is applied, k_B is Boltzmann's constant and T is the temperature.

For concreteness, assume that the dissipation in the fiber occurs through structural damping (our conclusions will hold equally well for viscous or thermoelastic damping). In this case, the average power dissipated during the oscillatory motion of frequency f is given by [8]

$$W_{diss} = 2\pi f U_{max} \phi(f), \tag{B6}$$

where U_{max} is the energy of the fiber's elastic deformation at a moment when it is maximally bent under the action of the oscillatory force in Eq. (B4), and $\phi(f)$ is the "loss angle" of the material. The energy of the fiber's elastic deformation is given by

$$U = \frac{JE}{2} \int_0^l dz \, [y'']^2 \, , \tag{B7}$$

where E is the Young modulus of the fiber material, J is the geometric moment of inertia of the fiber (for a fiber with circular cross section of diameter d one has $J = \pi d^4/64$), z is distance along the fiber with $z = 0$ at the top and $z = l$ at the bottom, and $y(z)$ is the fiber's horizontal displacement from a vertical line.

This method of calculating thermal noise is useful for a qualitative analysis of the system, as well as quantitative analysis. In particular, it allows one to see which part of the

---

mation when dealing with suspension thermal noise. The case when the test masses are no longer considered to be rigid (e.g. for an internal thermal noise calculations) is treated in detail in [7]. In that case the force $F(t)$ must be spread out over the laser beam spot instead of applied to it's center point.

suspension fiber contributes the most to the thermal noise. Assume, for a start, that the laser beam is positioned exactly in the middle of the mirror. Then to work out the thermal noise one has to imagine applying the oscillating force F in Eq. (3) to the mirror center; the motion of the fiber and the mirror under the action of the force are shown in Fig. 2a. Here we assume that the detection frequency f (and hence the frequency of the applied force) satisfies $f_p, f_r << f << f_v$, where f_p, f_r, f_v are the frequencies of the pendulum, rocking and first violin mode respectively (this condition implies that horizontal and rotational motion of the test mass is not affected by the presence of the fiber, and that the fiber itself remains straight).

From Fig. 2a it is clear that the fiber bends equally at the top and the bottom (we always assume that at the attachment point the fiber has to be normal to the surface to which it is attached). The total energy of elastic deformation is

$$U_0 = \frac{1}{2} Mg\lambda\alpha^2 = \frac{Mg\lambda}{2}\left(\frac{F}{M\omega^2 l}\right)^2, \tag{B8}$$

where $\lambda = \sqrt{JE/Mg}$ is the characteristic length over which the fiber is bent near the attachment points, $\omega = 2\pi f$ is the angular frequency of detection, and α is the angle between the straight part of the fiber and the vertical.

The bending of the fiber at the bottom can be avoided if one applies the force F in Eq. (B4) not at the middle of the mirror, but at some distance h below the center. In particular, we should choose h so that the mirror itself rotates by the same angle as the fiber under the action of the applied force; the resulting motion is shown on Fig. 2b. Physically this means that if we position our laser beam at a distance h below the mirror center, then the bottom attachment point will not contribute to the thermal noise when h is carefully chosen. This means that the overall suspension noise will be reduced by a factor of order 2 (in fact, more precisely, by a factor of $2(1 + R/l)$, where R is the radius of the mirror and l is the length of the string, — see later in this section).

In the rest of this section and Appendix I we find the general expression for the suspension thermal noise, and we then work out the optimal h for the frequency band of interest for

LIGO. We will assume that when a periodic oscillation of frequency f is induced in the system, the average power dissipated as heat in the suspension is given by

$$W_{\rm diss} = f\left[\zeta_{\rm top}(f)\bar{\alpha}_{\rm T}^2 + \zeta_{\rm bottom}(f)\bar{\alpha}_{\rm B}^2\right]. \tag{B9}$$

Here $\bar{\alpha}_{\rm T}$ and $\bar{\alpha}_{\rm B}$ are the amplitudes of oscillations of the angles $\alpha_{\rm T}$ and $\alpha_{\rm B}$ respectively (see Fig. 1), and $\zeta_{\rm top}$ and $\zeta_{\rm bottom}$ are frequency-dependent quantities characterizing dissipation at the top and the bottom respectively. For the case of structural damping

$$\zeta_{\rm top} = \zeta_{\rm bottom} = \pi f \phi(f) Mg\lambda, \tag{B10}$$

where λ is given by Eq. (B3) of the introduction.

To compute $W_{\rm diss}$ we need to evaluate $\bar{\alpha}_{\rm T}$ and $\bar{\alpha}_{\rm B}$ by analyzing the dynamics of the oscillations. This is done in Appendix I, see Eqs. (B40) and (B39). Putting these equations into Eq. (B9) and then into Eq. (B5), we obtain [cf. Eq. (B41)]

$$S_{\rm x}(f) = \frac{8k_{\rm B}T}{\omega^2}\left\{\frac{I/M - R(g/\omega^2+h)}{[Ig - MgR\,(g/\omega^2 - R)]\cos(kl) - (I\omega^2 - MgR)\sin(kl)/k}\right\}^2$$
$$\times\left\{\zeta_{\rm top} + \zeta_{\rm bottom}\cos^2(kl)\left[\frac{I/M - h\,[R + \tan\,(kl)\,/k - g/\omega^2]}{I/M - R(g/\omega^2+h)}\right]^2\right\}. \tag{B11}$$

Here $k = \omega/c = 2\pi f/c$, $c = \sqrt{glM/m}$ is the speed of propagation of a transverse wave in the fiber. From the above equation we can infer the ratio of the bottom and the top contributions to the thermal noise:

$$\frac{S_{\rm bottom}(f)}{S_{\rm top}(f)} = \frac{\zeta_{\rm bottom}(f)}{\zeta_{\rm top}(f)}\cos^2(kl)\left[\frac{I/M - h\,[R + \tan\,(kl)\,/k - g/\omega^2]}{I/M - R(g/\omega^2+h)}\right]^2. \tag{B12}$$

This is the most important equation in this section of the paper; it will be discussed in the next subsection.

3. The case of low-frequency suspension noise

When the detection frequency f is far below the frequency of the fundamental violin mode, $f_{\rm v}$, then $kl \ll 1$ in Eq. (B12) and

$$\frac{\tan(kl)}{k} \simeq l\left[1+\frac{1}{3}(kl)^2\right]. \tag{B13}$$

Let us assume that the top and the bottom are equally lossy, i.e. $\zeta_{\rm top} = \zeta_{\rm bottom}$, as the would be for structural damping, Eq (B10) above. We choose h to be

$$h = \frac{I}{M(R+l)}. \tag{B14}$$

Putting Eqs (B14) and (B13) into Eq. (B12), we get

$$\frac{S_{\rm bottom}(f)}{S_{\rm top}(f)} \simeq \frac{\pi^4}{9}\frac{1}{\left[1-(R/h)(\omega_p^2/\omega^2)\right]^2}\left(\frac{f}{f_{\rm v}}\right)^4, \tag{B15}$$

where $\omega_p = \sqrt{g/l}$.

For the initial and enhanced LIGO design $f_{\rm v} \simeq 400$Hz, $M \simeq 10$kg, $I \simeq 4.73\times10^{-2}{\rm kg}\times{\rm m}^2$, $R \simeq 12.5$cm, and the interesting frequency range where suspension noise is expected to dominate is $35-100$Hz (actually, this depends on the stage of enhancement. The frequency band specified above is where the suspension thermal noise is expected to dominate in the initial LIGO; in the enhanced version this frequency interval will be larger). In this case Eq. (B15) gives $S_{\rm bottom}(f)/S_{\rm top}(f) \simeq 0.002-0.2$.

In Fig.3 we give plots for $S_{\rm bottom}/S_{\rm top}$ as a function of the detection frequency f for three different choices of h. We have used Eq. (B15) to make all the plots and we set I, M, R and l to the numerical values appropriate for the initial and enhanced LIGO design and given at the beginning of this section.

The first curve is plotted for h given by Eq. (B14), in our case $h = 1.11$cm. The second and third curves are for $h = 1.0$cm and $h = 0.9$cm ; these values of h are chosen so that $S_{\rm bottom}/S_{\rm top} = 0$ for $f = 80$Hz and $f = 105$Hz respectively. Out of the three cases the choice $h = 1$cm gives the best overall performance across the considered frequency band, with the typical reduction factor of

$$\frac{S_{\rm bottom}}{S_{\rm top}} \sim 10^{-2}. \tag{B16}$$

¿From Eq. (B11) we see that choosing h close to the value in Eq. (B14) reduces the total suspension thermal noise by a factor close to $2(1+R/l) \sim 3$ relative to the case when $h = 0$.

4. High-frequency suspension thermal noise

A somewhat less interesting observation is that for $h = 0$ and $f_{\rm n} = f_{\rm v}(n + 1/2)$, where n is an integer,

$$\frac{S_{\rm bottom}(f_{\rm n})}{S_{\rm top}(f_{\rm n})} = 0. \tag{B17}$$

Unfortunately, at $f = f_{\rm n}$ the interferometer's noise is dominated by shot noise. However, if one uses an advanced optical topology — for example, resonant sideband extraction — then it is possible to reduce the shot noise in a narrow band around any chosen frequency. Then the thermal noise may dominate in this narrow band, and our observation (B17) may be useful in case one tries to reduce the thermal noise by cooling of the fiber top.

5. How to control noise from the top

a. The concept

In this section we propose a recipe for how to decrease the influence of the thermally fluctuating stress at the top part of the suspension fiber. The basic idea is the following:

Intuitively, the fluctuations at the top cause bending of the fiber at the top, which will be a random process in time. This random bending will randomly move the rest of the fiber and ultimately drive the random motion of the test mass. We propose to measure directly the thermally driven fluctuations in the horizontal displacement of the fiber, and from them infer the fluctuating force which drives the random motion of the mirror. We can then subtract the motion due to this fluctuating force from the interferometer output[5].

Formally this amounts to introducing a new readout variable q as follows:

$$q = X_{\rm mirror} + X_{\rm fiber}. \tag{B18}$$

---

[5]The idea of thermal noise compensation is not new (e.g. [11], [10]). However, our detailed treatment and concrete experimental proposal is different from anything prior to this paper.

Here $X_{\rm mirror}$ is the horizontal displacement of the laser spot's center (i.e.the signal ultimately read by the interferometer's photodiode), and

$$X_{\rm fiber} = \int_0^l dz \Phi(z) y(z) \tag{B19}$$

is the fiber's horizontal displacement weighted by some function $\Phi(z)$ to be discussed below. We will postpone the discussion of how to measure q experimentally until the next section; here we concentrate on finding the optimal $\Phi(z)$ and seeing what is the maximal possible reduction in the thermal noise.

To find the spectral density of fluctuations in q we need to imagine acting on the system with sinusoidal force $F_q \propto \cos(2\pi f t)$ that appears in the interaction hamiltonian in the following way

$$H_{\rm int} = -qF_q = -X_{\rm mirror}F_q - \int_0^l dz F_q \Phi(z) y(z); \tag{B20}$$

cf. the discussion of the Fluctuation-Dissipation theorem in Ref. [7]. From the Eq. (B20) we observe that applying the generalized force F_q to the system is equivalent to applying two forces simultaneously: one is a force of magnitude F_q applied to the mirror surface at the center of the beam spot, and the other is a force distributed along the fiber in the following manner:

$$\frac{dF_{\rm fiber}}{dz} = F_q \Phi(z). \tag{B21}$$

The resulting motion of the system is shown in Fig. 4. The intuitive idea is to choose the weighting function $\Phi(z)$ so that when the beam spot's height h has also been appropriately chosen, F_q induces no bending of the fiber at the top or at the bottom.

In the case of structural damping the dissipated power is proportional to the elastic energy U of the fiber. Thus formally one has to choose $\Phi(z)$ and h so that U is minimized. It is convenient to reformulate the problem: to find the shape of the fiber $y(z)$ and beam-spot height h for which the functional in Eq. (B7) has a minimum, and after this calculate the distribution $\Phi(z)$ of the driving force on the fiber that will produce the desired shape $y(z)$.

In Appendix II we carry out this straightforward but somewhat tedious task. We obtain [cf. Eq. (B50)]

$$y_{\rm optimal}(z) = \frac{F_q}{M\omega^2}\left(\frac{z}{l}\right)^2\left(\frac{3(r+1)-z/l}{2(3r^2+3r+1)}\right)$$
$$\simeq \frac{F_q}{M\omega^2}\left(\frac{z}{l}\right)^2\left(0.76-0.18\frac{z}{l}\right). \qquad \text{(B22)}$$

Here $r = R/l$, R is the radius of the mirror, l is the length of the fiber, $\omega = 2\pi f$ is the angular frequency of detection. We substitute here and below $r = 0.42$ corresponding to the initial and enhanced LIGO test masses. The profile of the distributed force acting on the fiber and hence of $\Phi(z)$ is mainly determined by $y''(z)$ (see Appendix II):

$$\Phi(z) \simeq \Phi_0 = -\frac{Mg}{F_q}y''(z), \qquad \text{(B23)}$$

which gives [cf. Eq. (B53)]

$$\Phi_0(z) \simeq -\frac{\omega_p^2}{\omega^2 l}\left(1+r-\frac{z}{l}\right)\frac{3}{3r^2+3r+1}$$
$$= -\frac{\omega_p^2}{\omega^2 l}\left(1.53-1.08\frac{z}{l}\right), \qquad \text{(B24)}$$

where $\omega_p = \sqrt{g/l}$. When the force distribution has this optimal form, the elastic energy has the minimum value

$$U_{\rm min} \simeq \frac{3}{3r^2+3r+1}\frac{\lambda}{l}\frac{Mg\lambda}{2}\left(\frac{F_q}{M\omega^2 l}\right)^2$$
$$= \frac{1.08\lambda}{l}\times U_0, \qquad \text{(B25)}$$

where U_0 is the elastic energy in Eq. (B8). Therefore, for a fused silica fiber with $E \simeq 6.9\times 10^{10}$Pa and $d = 0.6$mm, we get $\lambda \simeq 2.1$mm and the maximal reduction factor for the spectral density of suspension thermal noise is

$$P = \frac{l}{1.08\lambda} \simeq 132. \qquad \text{(B26)}$$

6. Experimental realization–a proposal

a. Preliminary remarks

Before describing a particular experimental realization of the above scheme, a few general remarks are in order.

First, one might worry that our averaging function $\Phi(z)$ is frequency dependent — in general, that could make the experimental implementation very difficult. In particular [see Appendix II, Eq.(B52)], Φ consists of two components: $\Phi = \Phi_0 + \Phi_1$, where Φ_0 and Φ_1 as given by Eq. (B52) have very different frequency dependence. However at the frequencies of interest $\Phi_0 \gg \Phi_1$, and then the approximate formula (B24) for the averaging function $\Phi(z) = \Phi_0(z)$ is a product of two terms: one which depends only on the frequency f (i.e. $\Phi(z) \propto 1/f^2$), and the other which depends only on the coordinate z. This feature makes the scheme feasible for a broad range of frequencies. It is sufficient that our device measures the displacement of the fiber with the frequency-independent averaging function $\tilde{\Phi}(z) \propto f^2 \times \Phi(z)$, and that the frequency dependence is then put back in during data analysis when constructing the readout variable q:

$$q = X_{\rm mirror} + \eta(f) \int_0^l dz \tilde{\Phi}(z) y(z), \tag{B27}$$

where $\eta(f) \propto f^{-2}$ is chosen so that $\eta\tilde{\Phi} = \Phi$.

As mentioned above, Eq. (B24) is an approximation valid when the fiber has no inertia, i.e. when $f \ll f_v =$ (lowest violin-mode frequency). When the inertia of the fiber becomes important ($\Phi_1 \sim \Phi_0$), it is no longer possible to factor out a frequency-dependent part of Φ. As a result, when f gets closer to f_v, the effectiveness of the thermal noise suppression (i.e. the value of P) is reduced. A detailed analysis shows that if we choose $\tilde{\Phi}(z)$ so that the thermal noise compensation is optimal ($P = P_{\rm max}$) at low frequencies $f \ll f_v$, then at $f = 0.2 f_v$ we have $P \sim 0.9 P_{\rm max}$, at $f = 0.32 f_v$ we have $P \sim 0.5 P_{\rm max}$, and beyond this P is reduced sharply as we approach the first violin mode. For the fused silica fiber discussed above $f_v \sim 400$Hz, so the compensation is effective throughout the band 35−100Hz

where suspension thermal noise dominates. It is worth emphasizing that this deterioration in the reduction factor only happens when we use the averaging function Φ_0 instead of $\Phi_0 + \Phi_1$ close to the violin frequency. Thus, this limitation is one of technology and not of principle. Perhaps, it is possible to conceive of a scheme where the correct averaging function is implemented at all frequencies. However, we have not been able to do so.

Secondly, any sensor used for monitoring the fiber coordinate $X_{\rm fiber}$ will have an intrinsic noise which will deteriorate the quality of the thermal-noise compensation. In particular, the overall reduction factor $P_{\rm eff}$ is given by

$$\frac{1}{P_{\rm eff}} = \frac{1}{P} + \frac{S_{\rm fiber\ meas}(f)}{S_{\rm fiber\ therm}(f)}, \tag{B28}$$

where $S_{\rm fiber\ meas}(f)$ is the spectral density of intrinsic noise of the device which measures the average displacement of the fiber and $S_{\rm fiber\ therm}(f)$ is the spectral density of thermal fluctuations of the same displacement.

For the case of structural damping it is easy to estimate

$$\sqrt{S_{X\ \rm fiber\ therm}(f) f} \sim \sqrt{\frac{\lambda \phi k T}{M g}} \sim 10^{-14}{\rm cm}, \tag{B29}$$

where we assume that $\phi \sim 10^{-7}$ for fused silica. If our goal is to achieve $P \sim 100$ then the condition $P_{\rm eff} \simeq P$ implies

$$\sqrt{S_{\rm fiber\ meas} f} << \sqrt{\frac{S_{\rm fiber\ therm} f}{P}} \sim 10^{-15}{\rm cm}. \tag{B30}$$

We shall take the above number as a sensitivity goal that our measuring device should achieve.

b. Proposed measuring device

Now we are ready to describe a possible practical implementation of our thermal-noise compensation scheme. Figure 5 illustrates the basic idea. We propose to use a fused silica optical fiber with the refractive index n_1 for the test mass's suspension. Next to this fiber we attach to the top seismic isolation plate (i.e. the "ceiling") a rigid block of the fused silica A

with the same index of refraction n_1. On the surface of this rigid block we put a thin optical waveguide with refractive index n_2 such that $n_2 > n_1$, so that the waveguide is at a distance $\sim \lambda_{\rm optical}/2\pi$ from the suspension fiber. It is assumed that the side of the waveguide close to the suspension fiber does not have any coating, i.e. it is "naked". In this configuration the optical wave may propagate through the waveguide without substantial scattering even though the suspension fiber is within the wave's evanescent zone. This device will produce a relatively large response to the displacement $X_{\rm fiber}$ in the form of a phaseshift of $\Delta\phi$ of the optical wave:

$$\Delta\phi = K \frac{2\pi X_{\rm fiber}}{\lambda_{\rm optical}} \frac{2\pi l}{\lambda_{\rm optical}}, \tag{B31}$$

where the dimensionless factor K depends on the values of n_1 and n_2 and for typical optical waveguides is $K \sim 10^{-3}$. Equation (B31) implies that in order to register $X_{\rm fiber} \sim 10^{-15}$cm we need a sensitivity $\Delta\phi \sim 10^{-7}$. Thus for averaging time of $\tau_{\rm grav} = 0.01$sec we need to use the power of coherent light of $W \sim 1$mW. This power can be decreased if one uses a resonant standing wave in the waveguide.

Apart from the shot noise of the laser light, let us briefly discuss two other kinds of noise in this sensor. A more complete discussion will be presented elsewhere.

The first kind is seismic noise. A simple calculation shows that the seismic contribution to the noise in the readout variable q is about twice as large in spectral density as the seismic contribution to the noise in $X_{\rm mirror}$. Thus the seismic noise will not be an issue at frequencies above the "seismic wall" of the LIGO sensitivity curve.

The second kind of noise we want to mention is the mechanical thermal fluctuations of the waveguide itself. Our estimates show that if these fluctuations are caused by structural damping (and not by some surface or contact defects), then the ratio of the mechanical thermal fluctuations of the waveguide to those of the fiber is

$$\frac{S_{\rm waveguide}}{S_{\rm fiber}} \sim \frac{Mg}{El\lambda} \sim 10^{-5}. \tag{B32}$$

Thus, if the system is sufficiently clean then the mechanical thermal fluctuations of the waveguide will probably not significantly reduce the sensitivity of our sensor.

It is worth noting that in order to achieve the optimal compensation of thermal noise, the distance $d(z)$ between the suspension fiber and the waveguide has to vary in accord with the optimal profile of the averaging function:

$$d = A - B \log [\Phi(z)] , \tag{B33}$$

where A and B are constants to be discussed elsewhere. In this case the phase of the waveguide's output records the optimally averaged coordinate $X_{\rm fiber}$ of the fiber.

The profile $d(z)$ may be difficult for experimental realization. However we find that in the simplest case when $\Phi(z)$ is a constant over the length l of averaging, the factor P is reduced very little: from $P = 132$ to $P \sim 120$.

7. Conclusion

In this paper we have done two things.

Firstly, we have shown that by an appropriate positioning of the laser's beam spot on the surface of each test-mass mirror, one can reduce the contribution of the suspension fiber's bottom to the suspension thermal noise by two to three orders of magnitude in the frequency band of $35 - 100$Hz for the initial LIGO design.

Secondly, we have proposed a way to compensate the suspension thermal noise originating from the top of each fiber by monitoring independently the fiber's random horizontal displacement. In the best case, with the system parameters for the initial or enhanced LIGO design, one can get a reduction factor of the order of $P = 130$ in spectral density over the entire $35 - 100$Hz band, when both the first and second procedures are applied; and with realistic defects in the design one should be able to get a reduction of at least $P \simeq 100$

The device that compensates the suspension thermal noise can ease the requirements to quality of suspension system. In particular, if this device allows the reduction factor of $P = 100$, this would effectively increase the quality factors of pendulum and violin modes by a factor of $P = 100$. So far the highest quality factor $Q \simeq 10^8$ of the pendulum

mode was achieved in [9] for a fused silica suspension fiber, which allows one to reach the Standard Quantum Limit for averaging time of 10^{-3}sec. Implementation of our proposal could effectively increase this quality factor to $Q_{\rm eff} \simeq 10^{10}$, which would reduce the thermal noise in LIGO to the level of Standard Quantum Limit for averaging time of 10^{-2}sec. Then the techniques which allow one to beat the Standard Quantum Limit (see e.g. [13]) could be used in the enhanced LIGO interferometers.

acknowledgments

We thank Sergey Cherkis, Michael Gorodetsky, Ronald Drever, Viktor Kulagin, Nergis Mavalvala, Peter Saulson and Kip Thorne for interesting discussions. We are grateful to Kip Thorne for carefully looking over the manuscript and making many useful suggestions. This research has been supported by NSF grants PHY-9503642 and PHY-9424337, and by the Russian Foundation for Fundamental Research grants #96-02-16319a and #97-02-0421g

Appendix I

In this appendix we solve the dynamical problem of finding the amplitudes $\bar{\alpha}_{\rm T}$ and $\bar{\alpha}_{\rm B}$ of oscillation of the top and bottom bending angles in Eq. (B9) when a periodic force

$$F = F_0 \cos(\omega t) \tag{B34}$$

is applied to the mirror at a distance h below the mirror center [we use these amplitudes in Eq. (B9) of the text]. For convenience we complexify all of the quantities:

$$F = F_0 e^{\imath\omega t}, \quad \alpha_{\rm T} = \bar{\alpha}_{\rm T} e^{\imath\omega t}, \quad \alpha_{\rm B} = \bar{\alpha}_{\rm B} e^{\imath\omega t},$$

$$x = \bar{x} e^{\imath\omega t}, \quad \psi = \bar{\psi} e^{\imath\omega t},$$

where x is the displacement of the test mass's center of mass and ψ is the angle by which the mirror is rotated (see Fig. 1) under the action of the force $F(t)$. As usual, $\omega = 2\pi f$ is the angular frequency.

¿From the projection of the Newton's Second Law on the horizontal axis we have

$$F_0 - (\bar{\alpha}_{\rm B} - \bar{\psi})Mg = -M\omega^2\bar{x}, \tag{B35}$$

and, for the rotational degree of freedom, the equation of motion is

$$F_0 h + MgR\bar{\alpha}_{\rm B} = I\omega^2\bar{\psi}, \tag{B36}$$

where R is the radius of the test-mass cylinder and I is the moment of inertia for rotation about the test-mass center of mass in the plane of the Fig. 1. In the two equations above we assume that $\alpha_{\rm B}$ and ψ are small.

The fiber's horizontal displacement y from a vertical line approximately satisfies the wave equation:

$$\frac{\partial^2 y}{\partial t^2} = c^2 \frac{\partial^2 y}{\partial z^2}, \tag{B37}$$

where z is distance along the wire, with $z = 0$ at the top and $z = l$ at the bottom, and $c = \sqrt{glM/m}$ is the transverse speed of sound in the wire. In this Appendix we use Eq. (B37) for flexible wire since it's solutions are simple. If one takes the stiffness into account this changes the solutions of Eq. (B37) by a relative order of λ/l, see e.g. [12]. However, when using Eq. (B37), we must allow non-zero bending angles at the top and bottom attachment points, $\alpha_{\rm T}$ and $\alpha_{\rm B}$. The energy of elastic strain of the wire then consists of two components: one from the bulk of the wire given by Eq. (B7), and the other from the bending at the attachment points given by Eq. (B8). The solution to Eq. (B37) is

$$y(z,t) = A\sin(kz)\, e^{i\omega t}, \tag{B38}$$

where $k = \omega/c$ is the wave vector of an off-resonance standing wave induced in the fiber and A is a constant. The boundary condition is set at the bottom by

$$\begin{aligned} A\sin(kl) &= \bar{x} + R\bar{\psi} \\ kA\cos(kl) &= \left(\bar{\alpha}_{\rm B} - \bar{\psi}\right). \end{aligned}$$

Putting these two equations into Eqs. (B35) and (B36), we find

$$\bar{\alpha}_{\rm B} = -F_0 \frac{I/M - h\left[R + \tan\left(kl\right)/k - g/\omega^2\right]}{MgR^2 + \left(I\omega^2 - MgR\right)\left[g/\omega^2 - \tan\left(kl\right)/k\right]} \tag{B39}$$

and

$$\bar{\alpha}_{\rm T} = -F_0 \frac{I/M - R(g/\omega^2 + h)}{\left[Ig - MgR\left(g/\omega^2 - R\right)\right]\cos(kl) - \left(I\omega^2 - MgR\right)\sin(kl)/k}. \tag{B40}$$

Putting Eqs. (B39), (B40) and (B9) into Eq. (B5), we finally get for the spectral density of the suspension thermal noise:

$$S_{\rm x}(f) = \frac{8k_{\rm B}T}{\omega^2}\left\{\frac{I/M - R(g/\omega^2 + h)}{\left[Ig - MgR\left(g/\omega^2 - R\right)\right]\cos(kl) - \left(I\omega^2 - MgR\right)\sin(kl)/k}\right\}^2 \left\{\zeta_{\rm top} + \zeta_{\rm bottom}\cos^2(kl)\left[\frac{I/M - h\left[R + \tan\left(kl\right)/k - g/\omega^2\right]}{I/M - R(g/\omega^2 + h)}\right]^2\right\}. \tag{B41}$$

Appendix II

Here we calculate the optimal shape $y_{\rm optimal}(z)$ of the fiber and the vertical position of the laser beam spot h that minimize the fiber's elastic deformation energy [Eq. (B7)].

It is easy to deduce from Eq. (B7) that energy minimizing function $y(z)$ obeys the equation $y''''(z) = 0$. Therefore

$$\frac{y(z)}{l} = a_0 + a_1\frac{z}{l} + a_2\frac{z^2}{l^2} + a_3\frac{z^3}{l^3}, \tag{B42}$$

where a_i are constants to be determined.

Let us discuss the boundary conditions. Strictly speaking, the boundary conditions should be such that the fiber is perpendicular to the surface of attachment at both the top and the bottom. Therefore at the top we have $y(0) = y'(0) = 0$, from which immediately follows $a_0 = a_1 = 0$. However, at the bottom it is more convenient for our calculations embody the bending of the fiber, on the lengthscale λ, in a bending angle $\alpha_{\rm B}$ as in Fig. 1, and correspondingly add an additional term

$$U_{\rm add} = (1/4)Mg\lambda\alpha_{\rm B}^2 \tag{B43}$$

to the energy functional in Eq. (B7), and then in Eq. (B42) evaluate $y(l)$ and it's derivatives above the λ-scale bend. Our energy minimization procedure will make the angle $\alpha_{\rm B}$ so small that the additional elastic energy as given by Eq. (B43) is negligible compared to U in Eq. (B7)

The coefficients a_2 and a_3 can be inferred from force and torque balance at the test mass:

$$F_q - Mgy'(l) = -M\omega^2(y(l) + R(y'(l) + \alpha_{\rm B})), \tag{B44}$$

and

$$F_q h - MgR\alpha_{\rm B} = -I\omega^2(y'(l) + \alpha_{\rm B}).$$

It is useful to rewrite these equations in a dimensionless form:

$$\begin{aligned} \xi(1 + \eta(r-a)) + r\alpha_{\rm B} &= -\xi_0, \\ \eta\xi + \alpha_{\rm B}(1 - \mu r a) &= -\mu s \xi_0; \end{aligned} \tag{B45}$$

where

$$\xi = \frac{y(l)}{l}, \quad \eta = \frac{y'(l)l}{y(l)}, \quad s = \frac{h}{l},$$

$$a = \frac{\omega_p^2}{\omega^2} \simeq 10^{-3} \ \div 10^{-6}, \quad r = 0.42, \quad \mu = \frac{Ml^2}{I} = 19,$$

where $\omega_p = \sqrt{g/l}$. Here we have used for estimates the mirror parameters for the initial and enhanced LIGO interferometers. Solving the above system of equations (B45) for ξ and $\alpha_{\rm B}$ (taking η as a parameter) we get:

$$\alpha_{\rm B} = \xi_0 \frac{\eta - \mu s(1 + \eta(r-a))}{[1 + \eta(r-a)][1 - \mu r a] - r\eta} \simeq \xi_0[\eta - \mu s(1 + \eta(r-a))]$$

$$\xi = -\xi_0 \frac{1 - \mu r(a+s)}{[1 + \eta(r-a)][1 - \mu r a] - r\eta} \simeq -\xi_0(1 - \mu r(a+s))$$

Let us choose the parameter s so that $\alpha_{\rm B} = 0$ for some angular frequency ω_0 in the frequency band $35 - 100$Hz where thermal noise is most serious:

$$s \simeq \frac{\eta}{\mu[1 + \eta(r - a_0)]} \simeq \frac{\eta}{\mu[1 + \eta r]}, \quad a_0 = \frac{\omega_p^2}{\omega_0^2} \tag{B46}$$

Then we get for $\alpha_{\rm B}$ and ξ

$$\alpha_{\rm B} \simeq \xi_0 \frac{\eta^2}{1+\eta r}(a-a_0) \tag{B47}$$

$$\xi \simeq -\xi_0 \frac{1}{1+\eta r}.$$

We can express the coefficients a_3 and a_2 in terms of ξ and η by combining Eqs. (B42) and (B45), and we can then calculate the elastic energy according to Eq. (B7):

$$U \simeq \frac{Mg\lambda}{2}\left(\frac{F_q}{M\omega^2 l}\right)^2 \times \frac{\lambda}{l} \times \frac{4(\eta^2-3\eta+3)}{(1+r\eta)^2} \tag{B48}$$

This function has the minimal value

$$U_{\rm min} \simeq \frac{l}{\lambda} \times \frac{3}{1+3r+3r^2} \times U_0 = \frac{1.08\lambda}{l} \times U_0$$

at optimal η given by

$$\eta_{\rm opt} = \frac{3(1+2r)}{2+3r} = 1.69. \tag{B49}$$

Here U_0 is the energy of elastic strain of the fiber when the force of magnitude F_q is applied in mirror center, as worked out in Eq. (B8). Now we can figure out the optimal shape of the fiber's horizontal displacement:

$$\begin{aligned} y_{\rm optimal}(z) &= \frac{F_q}{M\omega^2}\left(\frac{z}{l}\right)^2\left(\frac{3(r+1)-z/l}{2(3r^2+3r+1)}\right) \\ &\simeq \frac{F_q}{M\omega^2}\left(\frac{z}{l}\right)^2\left(0.76-0.18\frac{z}{l}\right). \end{aligned} \tag{B50}$$

From Eq. (B46) we get $h = l \times s \simeq 1.55$cm.

Using (B47) one can show that $\alpha_{\rm B} \leq 1.7 \cdot 10^{-3} \cdot \xi_0$ over the frequency band $35-100$Hz. From this and Eq. (B43), one can compute the energy due to the bending at the fiber bottom: $U_{\rm add} \simeq 1.4 \cdot 10^{-6} \times E_0$. We see that $U_{\rm add} \ll U_{\rm min}$ and hence over the frequency band of interest the small bending at the bottom does not contribute significantly to the total energy of elastic deformation.

The profile of the distributed force and correspondingly the function Φ are given by

$$F_q\Phi(z) = -\rho\omega^2 y(z) - Mgy''(z) + IEy''''(z). \tag{B51}$$

Here ρ is the fiber density per unit length. Since $y''''(z) = 0$, the function Φ consists of two terms $\Phi(z) = \Phi_0(z) + \Phi_1(z)$, where

$$\Phi_0(z) = -\frac{Mg}{F_q}y''(z), \quad \Phi_1(z) = -\frac{\rho\omega^2}{F_q}y(z). \tag{B52}$$

$$\Phi_0(z) = \frac{\omega_p^2}{l\omega^2}\cdot\left(1 + r - \frac{z}{l}\right)\cdot\frac{3}{3r^2+3r+1} = \frac{\omega_p^2}{l\omega^2}\cdot\left(1.53 - 1.08\frac{z}{l}\right). \tag{B53}$$

We see that Φ_0 is much greater than Φ_1 in our frequency range ($10 - 100$Hz for the initial LIGO).

REFERENCES

[1] A. Abramovici *et. al.*, Science, **256**, 325 (1992); C. Baradaschia *et. al.*, Nucl. Instrum & Methods, **A289**, 518 (1990).

[2] B. Barish *et. al.*, "LIGO advanced Research and Development Program Proposal", LIGO technical document LIGO-M970107-00-M (Caltech, 1996).

[3] G. I. Gonzalez and P. R. Saulson, *J. Accoust. Soc. Am*, **96**, 207-212 (1994).

[4] N. Nakagawa *et. al.*, *Rev. Sci. Instrum.* **68(9)**, 1-4 (1997).

[5] A. V. Gusev *et. al.*, *Radiotekhnika i Elektronika*, **40**, 1353-1359 (1995).

[6] H. B. Callen and T. A. Welton, *Phys. Rev.* **83**, 3 4-50 (1951).

[7] Yu. Levin, *Phys. Rev. D*, **57**, 659-663 (1998) .

[8] P. R. Saulson, *Phys. Rev. D*, **42**, 2437-2445 (1990).

[9] V. B. Braginsky, V. P. Mitrofanov, K. V. Tokmakov, *Phys. Lett. A*, **218**, 164-166 (1996) and references therein.

[10] V. V. Kulagin, First E. Amaldi conference on grav. wave experiments, editors E.Coccia, G.Pizzella, F.Ronga, World Sci. Publ. Comp., 1995, p. 328..

[11] Remarks by R. Weiss and others in informal LIGO team discussions.

[12] L. D. Landau and E. M. Lifschitz, *Theory of Elasticity* (Pergamon Press, New York, 1986).

[13] At the moment there is no practical proposal to beat the Standard Quantum Limit which could be readily implemented in LIGO. However, conceptual schemes can be found in e.g.

A. V. Syrtsev and F. Ya. Khalili, JETP **79** (3), 409-413 (1994);

S. P. Vyatchanin and A. B. Matsko, Zh. Eksp. Teor. Fiz. v.110 (1996) 1253 (*English*

translation: JETP v.83(4), 690 (1996));

V. B. Braginsky, M. L. Gorodetsky, F. Ya. Khalili, Physical Letters A **A232**, 340-348 (1997)

and references therein.

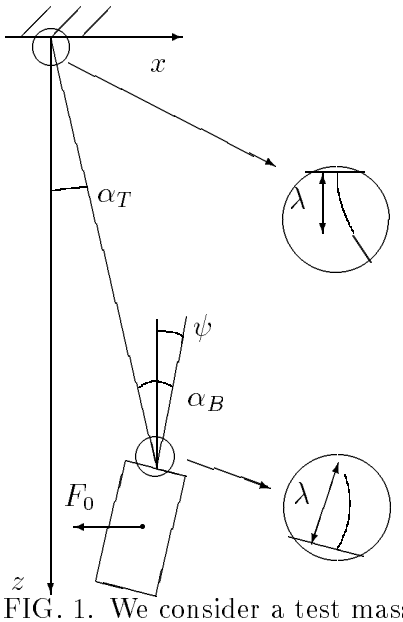

FIG. 1. We consider a test mass suspended on a single fiber. The fiber's bottom is attached to the top of the test mass, and the fiber's top is attached to the last stage of the seismic isolation stack. It is assumed that at attachment points the fiber is perpendicular to the surface to which it is attached.

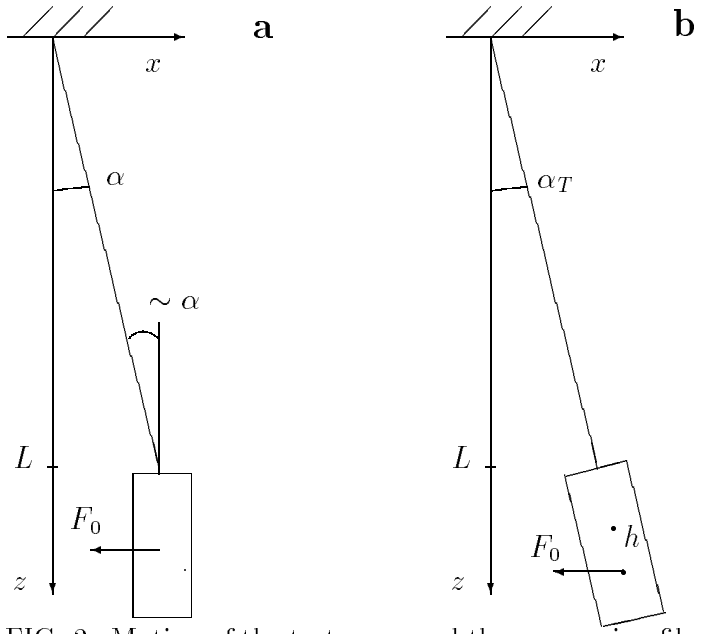

FIG. 2. Motion of the test mass and the suspension fiber under the action of an oscillating force applied at the center of the laser beam spot in two different cases: *a)* the beam spot is positioned at the mirror center, the fiber bends equally at the top and the bottom, and *b)* the position of the beam spot is shifted down from the center of the mirror, so that there is no bending of the fiber at the bottom.

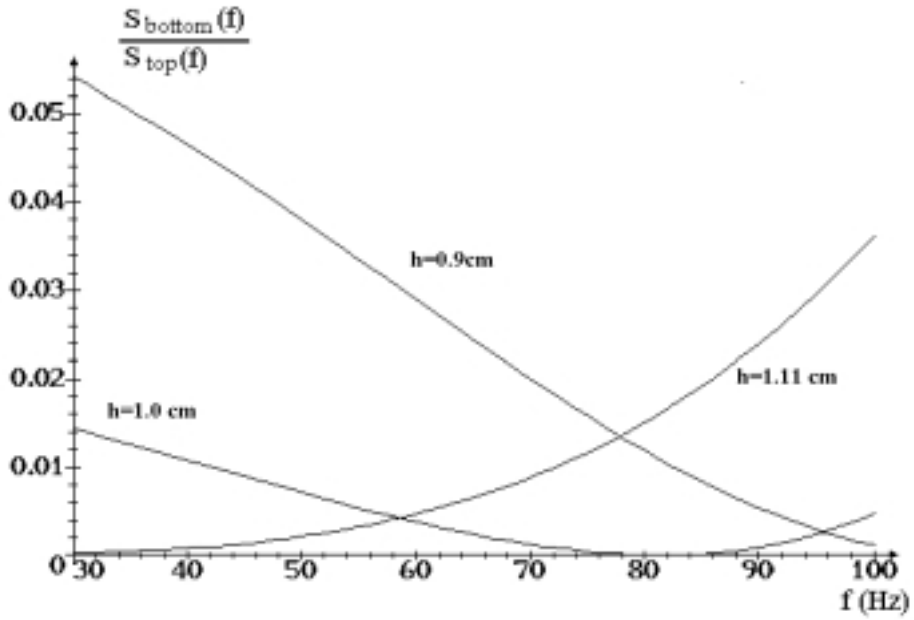
S bottom (f)
S top (f)
0.05
0.04
0.03
0.02
0.01
0
30
40
50
60
70
80
90
100
f (Hz)
h=0.9cm
h=1.11 cm
h=1.0 cm

FIG. 3. A plot of $S_{\mathrm{bottom}}(f)/S_{\mathrm{top}}(f)$ as a function of frequency f for three different positions of the laser beam spot.

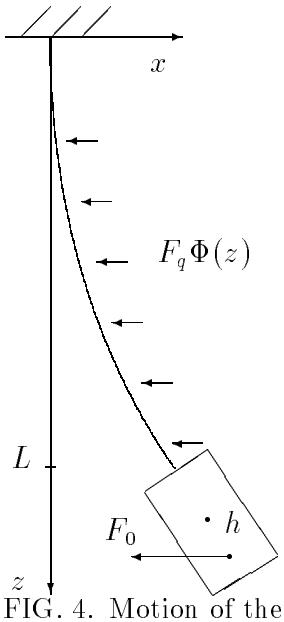

FIG. 4. Motion of the test mass and suspension fiber under the action of the generalized force F_q defined in Eq. (B20) of the text. The force F_q should be chosen so that there is no bending of the fiber at it's top and bottom attachment points.

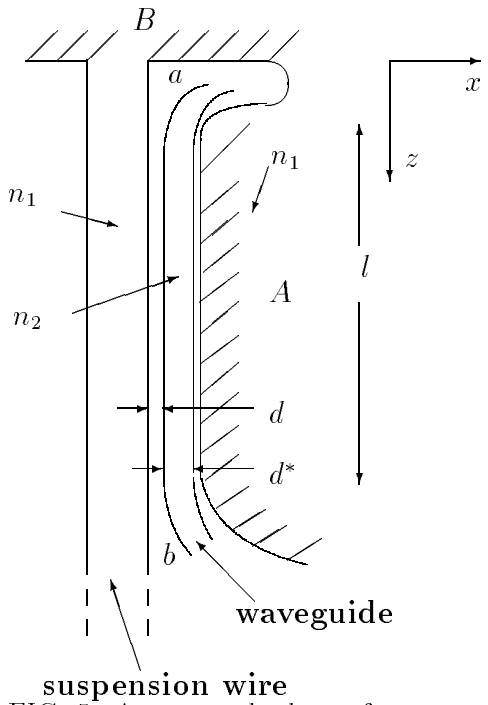

FIG. 5. A proposed scheme for compensation of a suspension thermal noise. The optical waveguide ab is positioned close to the suspension fiber made of fused silica. A horizontal displacement of the suspension fiber is recorded through a phase shift of an optical wave propagating through the waveguide.